IEEE Access
Multidisciplinary ⋮ Rapid Review ⋮ Open Access Journal

Received 8 November 2023, accepted 28 November 2023, date of publication 30 November 2023,
date of current version 12 December 2023.

Digital Object Identifier 10.1109/ACCESS.2023.3338540

RESEARCH ARTICLE

Classification of Dead Cocoons Using Convolutional Neural Networks and Machine Learning Methods

AHYEONG LEE[1], GIYOUNG KIM[1], SUK-JU HONG[1], SEONG-WAN KIM[2], AND GHISEOK KIM[3,4,5]

[1]Department of Agricultural Engineering, National Institute of Agricultural Sciences, Deokjin-gu, Jeonju 54875, Republic of Korea
[2]Department of Agricultural Biology, National Institute of Agricultural Sciences, Iseo-myeon, Wanju 55365, Republic of Korea
[3]Integrated Major in Global Smart Farm, Seoul National University, Gwanak-gu, Seoul 08826, Republic of Korea
[4]Department of Biosystems Engineering, College of Agricultural and Life Sciences, Seoul National University, Gwanak-gu, Seoul 08826, Republic of Korea
[5]Research Institute of Agriculture and Life Science, College of Agriculture and Life Sciences, Seoul National University, Seoul 08826, South Korea

Corresponding author: Ghiseok Kim (ghiseok@snu.ac.kr)

This work was supported by the Research Program for Agricultural Science & Technology Development (Project No. PJ01586801), National Institute of Agricultural Science, Rural Development Administration, Republic of Korea.

ABSTRACT Image recognition methods classify or categorize objects by extracting significant properties from digital images of the objects and are used in the field of agriculture for quality determination. With the development of artificial intelligence technology, deep-learning techniques and tools such as convolutional neural networks (CNNs) have been used in image recognition. Existing discrimination studies have tended to extract features from images and classify them using multivariate analysis; however, deep learning algorithms have the self-learning ability to extract the feature points themselves for each neural layer. In this study, we developed models for discriminating dead cocoons using various discriminant analysis methods, including deep learning options, to establish an automation technology for the sericulture industry. A 100 W halogen light source was used for direct irradiation onto the cocoons, and a camera was positioned at the bottom of the cocoons (of which 43.9% were dead) to obtain RGB images. We conducted discrimination analyses based on the color space using four discrimination algorithms, namely, k-nearest neighbor, support vector machine, linear discriminant analysis, and partial least squares-discriminant analysis, within deep learning models (a proposed lightweight CNN model, VGG16, ResNet50, EfficientNetB0, MobileNet, ShuffleNet, GhostNet, and ConvNext). The proposed lightweight CNN model, which consisted of six convolutional layers and two fully connected layers, showed the highest discrimination accuracy (97.66%) in the Lab color space. It was thus confirmed that it is possible to automate the discrimination of dead cocoons using digital images and deep learning techniques.

INDEX TERMS Convolutional neural networks, machine learning, discrimination, cocoon.

I. INTRODUCTION

A digital image is a digital representation of an analog image for digital computer analysis. Digital images have superior image quality compared to analog ones and various image processing techniques can be utilized to process digital data, and because of these advantages, research on image processing using digital images has been continuously developing. Digital image recognition is a digital image processing technology that can classify or categorize objects by extracting their significant properties [1]. Image recognition is mainly used in the field of quality discrimination as an alternative to the operator's visual selection process. Existing quality discrimination studies typically focus on techniques for selecting a region of interest from the acquired image using various channels, extracting the colors, and classifying the objects in the images into classes using multivariate analyses [2], [3]. With the development of artificial intelligence technology, high-performance CPUs and GPUs have been developed, and vast amounts of learning data is publicly available. Therefore, the applicability of deep learning is expanding to fields such as image and voice recognition [4].

The associate editor coordinating the review of this manuscript and approving it for publication was Utku Kose.

Deep learning is a machine learning method that uses an artificial neural network consisting of several hidden layers between the input and output layers [5]. An artificial neural network is a processor based on neuroanatomical facts. These networks were developed by cognitive scientists and researchers interested in new computational models and their structure is similar to the multiple neural layers found in the visual cortex of the brain. General image processing technologies determine the data class by extracting features from images and learning them based on the feature values. Image processing technology based on deep learning models however, does not require human intervention in the feature extraction process but has the self-learning ability to extract the feature points for each neural layer itself [6], [7]. Among the various deep learning models available, convolutional neural networks (CNNs) are mainly used to classify images of people, cars, and animals [8], [9], [10]. Ko et al. [11] proposed a six-step tomato ripeness classification system using RGB images and CNN algorithms with an accuracy of 91.3%. The results showed that the discrimination performance was higher in terms of the dataset size and complex maturity level compared with those of existing learning models, which extract features based on the statistical characteristics of the data. Fan et al. [12] used a four-line sorting machine capable of sorting five apples per second and developed a model to detect defective apples using a support vector machine (SVM) and deep learning technology based on CNNs. The classification accuracy of the SVM classifier was 87.1%, and the CNN classifier achieved a discrimination accuracy of 92% with a processing time of less than 72 ms for six images of one apple; these results confirm the superiority of the deep learning algorithm. Given these advantages deep learning technology is being used in various fields such as the quality assessment of agricultural products, classification of crop varieties [13], [14], diagnosis of growth status [15], [16], insect recognition and classification for agricultural pest removal [17], [18], and grading of livestock products [19], [20].

The sericulture industry currently exists in 25 countries worldwide and is economically significant in most developing countries [21], [22]. Silk production is the primary objective of the industry and the production of high-quality silk cocoons has become more significant with the development of high-value-added applications such as healthy functional foods [23], [24], functional products [25], [26], and medical materials based on sericulture by-products [27], [28], [29]. Dead cocoons have no commercial value and cause the cross-contamination of normal cocoons and therefore detection and removal of these dead cocoons is crucial. It is thus necessary to sort them before distribution, this sorting process having a determining effect on the price of the cocoons [30]. In the case of dead cocoons, the external defects of the cocoons can be identified using standard photos; sorting dead cocoons with internal defects is a different challenge [31]. Current methods see workers at the reeling center shake the cocoons one by one or sort them under sunlight because dead cocoons usually make no sound when shaken and appear black when exposed to sunlight [30], [32]. Development of technology that allows for the automatic identification of dead cocoons is therefore necessary for the automation of the sericulture industry.

Several studies on the use of image processing technology in the sericulture industry have been reported [33], [34], [35]. Tao et al. [36] used the radial basis function and neural network and SVM models to classify the sex and species of 840 silkworm pupae with 100% accuracy. Zhu et al. [37] measured the near-infrared spectra (899–1721 nm wavelength band) of 1600 silkworm pupae and developed a soft independent modeling of class analogy model to discriminate their sex with 98.8% accuracy. With respect to detecting dead cocoons, Zheng [38] imaged 100 cocoons and then separated the regions corresponding to the cocoons and the background using binarization. They could determine whether the cocoons were defective or not with an average accuracy of 98%. Prasobhkumar et al. [39] imaged 137 cocoons using a mobile phone camera and used the images to categorize normal cocoons and four types of dead cocoons, at a rate of 96 samples per second, using image processing methods based on binarization and morphology-related operations. Feng et al. [40] acquired 13514 images of five types of dead cocoons and developed an AlexNet with a global average pooling layer to classify the cocoons with an average accuracy of 98.22%. Sun et al. [41] developed an algorithm for segmenting eight types of dead cocoons based on VGG19. They proved that the image segmentation speed and accuracy were faster and higher, respectively, than those of the existing threshold-based segmentation algorithm. Thus, several studies have reported high-accuracy discriminating systems for identifying dead cocoons. However, these studies only evaluated dead cocoons with external defects. In addition, the models were developed using conventional image processing methods.

To overcome these limitations, we have developed a cocoon-discrimination model to identify dead cocoons with no external defects. Cocoons were radiated by a halogen light from above and then imaged from the bottom using a DSLR camera to capture their internal characteristics. The discrimination model for the dead cocoons was developed using several classification algorithms (k-nearest neighbor (k-NN), SVM, linear discriminant analysis (LDA), and partial least squares-discriminant analysis (PLS-DA)) and deep learning models. The deep learning models included a proposed lightweight CNN model. Furthermore, VGGNet, ResNet, EfficientNet, MobileNet, ShuffleNet, GhostNet, and ConvNext which are state-of-the-art deep learning models and widely used for image classification, were used. The most suitable algorithm for determining dead cocoons was selected by calculating and comparing the classification accuracy for each model.

The main contributions of this paper are as follows:

1) We propose an imaging acquisition method which can capture the internal structure of a cocoon without cutting.

By radiating the light from above, our imaging system captures the internal structure of cocoons. This imaging system can be used to replace labor force.

2) In this paper, we propose a lightweight CNN model to discriminate dead cocoons. This model was compared with the state-of-the-art deep learning models. The model exhibited the highest discrimination performance and is suitable for integration into sorting devices.

3) The results of this study contribute to the development of automation technology in the sericulture industry.

II. MATERIALS AND METHODS

A. INSTRUMENTATION AND DATA ACQUISITION

A total of 1,066 cocoons were supplied for the study by the Industrial Insect and Sericulture Division, Department of Agricultural Biology, Rural Development Administration, Korea, and a sericulture farm in Yeongdeok-gun, Gyeongsangbuk-do, Korea. The cocoons were stored in a controlled-atmosphere room with a temperature and humidity of 24 °C and 60%, respectively. As shown in Fig. 1, a digital imaging system was used to acquire the images of the cocoons. The pupae within the cocoons have the property of being located below by gravity. Based on this fact, a 100 W halogen light (LS-F100HS, Seokwang Optical Co., Korea) was radiated on the upper part of the cocoon sample to confirm the shape of the pupae within them. The images were obtained by placing a DSLR camera (Camera: E0S 5Ds, Canon, Japan, Lens: 24–70 mm ultrasonic, Canon, Japan) under the cocoons. The distance between the camera and the cocoon was consistently maintained at 50 cm. All experiments were conducted in black room to prevent further optical interference. After obtaining the images, the cocoons were cut to determine whether the pupae inside were dead. It was found that 598 of the cocoons were normal and 468 were dead.

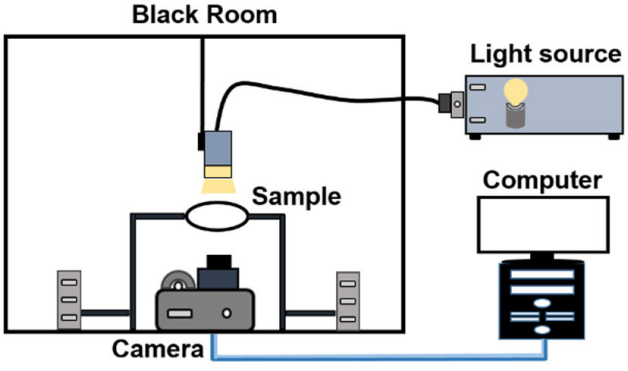

FIGURE 1. Schematic of digital imaging system for cocoon images.

B. IMAGE PREPROCESSING

As shown in Fig. 2, all the acquired images were preprocessed before being used to develop the dead-cocoon discrimination model. Fig. 2(a) is the original image and Fig. 2(b) is the cropped image showing the region of interest. Fig. 2(c) shows the background-subtracted image, in which the cocoon

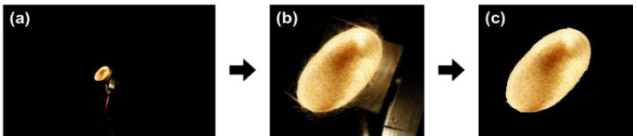

FIGURE 2. Digital image preprocessing method: (a) original, (b) cropped, and (c) background-subtracted images.

has been separated from the background in the image. The binarization process for this subtraction step was performed using the algorithm reported by Otsu [42], which converts the original image into grayscale and selects the appropriate threshold to maximize the between-class variance as calculated using (1). The algorithm was implemented using MATLAB (ver. 2022; MathWorks Inc., Natick, MA, USA), and images that were not properly binarized by Otsu's method were manually processed using Photoshop (Photoshop 7.0, Adobe Inc., USA).

$$\sigma_B^2 = w_0 w_1 (\mu_1 - \mu_0)^2 \tag{1}$$

where w_0 and w_1 are the probabilities of the occurrence of the two classes (background and object) and μ_0 and μ_1 are the means of the classes.

The original image data from DSLR cameras consist of RGB values. To identify the color channels suitable for silkworm cocoon discrimination the RGB color space was converted into HSV, Lab, and YCbCr color spaces and the four types of color spaces were used for analysis. The HSV color space defines the color of an image in terms of the hue, saturation, and value components. The hue and saturation components describe the changes in the chromaticity, while the Lab color space uses the L component to indicate the luminance or brightness, the "a" component represents the amounts of red and green tones, and the "b" component represents the amounts of yellow and blue tones. In the YCbCr color space, the Y component represents the luminance, the Cb component represents the difference between the reference value and the blue component, and the Cr component represents the difference between the reference value and the red component. For each image, the average value for each channel in the color space for all the pixels was taken as the representative value. The t-test was used to confirm whether there was a significant difference in the color channels of the normal and dead cocoon groups

C. DISCRIMINANT ANALYSES

Statistical discrimination algorithms (widely used in existing classification models) and deep learning algorithms were used to detect the dead cocoons.

First, discriminant analyses were performed using the k-NN, SVM, LDA, and PLS-DA methods. The k-NN method classifies samples into classes with the closest distance based on the distance between the samples in the feature space. SVM separates the classes by finding the boundary that maximizes the distance between the support vectors for each group and the hyperplane. The LDA reduces the dimen-

sion of the feature vectors by maximizing the ratio of the variance between the classes and that within the classes. The PLS-DA is based on the partial least square regression (PLSR) method and performs classification based on a regression equation using the threshold value. The discrimination accuracy of the developed model was calculated using (2). Model training and validation were performed using five-fold cross-validation. The 1066 cocoon images were divided into five groups, of which four were used for model training, one used for model validation. The average of five discrimination performances was calculated and taken as the final discrimination accuracy.

$$Accuracy = \frac{TP + TN}{TP + FP + TN + FN} \tag{2}$$

where TP is true positive, FP is false positive, TN is true negative, and FN is false negative.

Next, eight different deep learning models (a proposed lightweight CNN model, VGG16, ResNet50, EfficientNetB0, MobileNet, ShuffleNet, GhostNet, ConvNext) were compared to select an appropriate discrimination model. The image input size was set to $224 \times 224 \times 3$.

Before training the deep learning models, data augmentation was implemented to increase the data size. Data augmentation was performed using a Keras module named ImageDataGenerator. The module was set with a rotation degree range of 40, width and height shift range of 0.2, shearing transformation range of 0.2, zoom range of 0.2, and horizontal flip ratio of 0.5. When the process is performed, the points that exceed the boundary are filled by the nearest pixel values. To perform model training and validation, 1066 images were randomly divided into a training group (60%, 639), validation group (20%, 213), and test group (20%, 214). The training group image increased by 16 times because of the data augmentation.

The first discrimination model is the proposed lightweight CNN model. The developed model consists of six convolution layers and two fully connected layers, as shown in Table 1. Initially, the structure of the lightweight CNN model was built based on the VGG16 model. The kernel size, stride, padding, and activation values were referenced from the VGG 16 model. We compared the performance of the model by changing the number of convolution layers from four to seven and observed that the highest performance was achieved using six convolution layers. Max pooling demonstrated a higher and stable performance than average pooling. Therefore, Convolution was performed with stride of 1 and max pooling was performed between each convolution layer. Furthermore, dropout was performed between each convolution layer to reduce the number of model parameters. A batch size of 16 and the Adam optimizer were selected for model optimization. When training the model, the epoch was repeated 3000 times. The model training was set to end when the loss of the validation group did not improve for more than 50 consecutive iterations. The loss was calculated using (3).

TABLE 1. Architectures of the proposed lightweight CNN.

Layer name	Output size	Specifications
Input	224×224×3	
Convolution1	224×224×32	kernel size=3×3, stride=1×1, padding=same, activation='relu'
Max pooling	112×112×32	kernel size=2×2
Dropout	112×112×32	rate=0.3
Convolution2	112×112×32	kernel size=3×3, stride=1×1, padding=same, activation='relu'
Max pooling	56×56×32	kernel size=2×2
Dropout	56×56×32	rate=0.3
Convolution3	56×56×32	kernel size=3×3, stride=1×1, padding=same, activation='relu'
Max pooling	28×28×32	kernel size=2×2
Dropout	28×28×32	rate=0.3
Convolution4	28×28×64	kernel size=3×3, stride=1×1, padding=same, activation='relu'
Max pooling	14×14×64	kernel size=2×2
Dropout	14×14×64	rate=0.3
Convolution5	14×14×64	kernel size=3×3, stride=1×1, padding=same, activation='relu'
Max pooling	7×7×64	kernel size=2×2
Dropout	7×7×64	rate=0.3
Convolution6	7×7×64	kernel size=3×3, stride=1×1, padding=same, activation='relu'
Max pooling	3×3×64	kernel size=2×2
Dropout	3×3×64	rate=0.3
Flatten	576	
Fully Convolution	2048	activation='relu'
Fully Convolution	256	activation='relu'
Fully Convolution	2	activation='sigmoid'

$$Loss = -\frac{1}{N}\sum_{i=1}^{N} y_i \log(\widehat{y_i}) + (1-y_i) log(1-\widehat{y_i}) \tag{3}$$

where N is total number of data points, y_i is the real value, and $\widehat{y_i}$ is the predicted value.

VGG16, ResNet50, EfficientNetB0, MobileNet, ShuffleNet, GhostNet, ConvNext were the seven discrimination models that were compared with the proposed model. The performances of these existing models were demonstrated by an image classification competition. Therefore, we used these models for transfer learning and compared their performance with that of the proposed lightweight CNN model. These models were pre-trained by ImageNet. However, our image data differed from the data on ImageNet. Therefore, we used only the structure of the models and fine-tuned the models by training using our image. The hyperparameters, such as batch size, optimizer, epoch used for training the models were equal to that of the lightweight CNN.

Deep learning modeling was conducted using four color spaces (RGB, Lab, HSV, YCbCr) and the model with the highest discriminant accuracy was selected as the discrimination model for this study.

All the discriminant analyses were performed using Python (V3.8, Python Software Foundation, USA). For the calculations, a computing system equipped with a CPU (Ryzen 9 3900X, AMD, USA), 64 GB RAM, and a GPU (RTX 2080 Ti, Nvidia Corporation, USA) was used.

III. RESULTS AND DISCUSSION

A. FEATURES OF COCOON IMAGES

As previously mentioned, a total of 1066 cocoon images were acquired. Fig. 3 shows some of the obtained images of normal and dead cocoons. In the case of the normal cocoons the pupae in the cocoon are mostly brown and oval. In addition, a peeled silkworm shell is created as the silkworm transforms into a pupa. Therefore, in some of the images, the shells and pupae appear together.

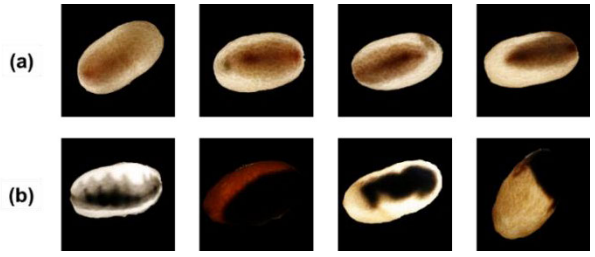

FIGURE 3. Representative cocoon images used in modeling: (a) normal cocoon and (b) dead cocoon with no external defects.

The dead cocoons were generally darker in color compared to the normal cocoons, and some were even close to black in color. Here, the term "dead cocoon" refers to all the cases in which the silkworm did not pupate within the cocoon. For example, there were cases that included specimen death in the form of silkworm larva, death during pupal metamorphosis, or the pupa bursting and contaminating the inside of the cocoon. Therefore, various internal shapes were observed in the images of the dead cocoons, in contrast to that of the normal cocoons. It was therefore assumed that it would be possible to discriminate the dead cocoons by appropriately extracting their features from the acquired images.

Fig. 4 shows box plots of the normal and dead cocoon groups for each channel in the four color spaces. For the RGB color space, the average values of the normal and dead cocoons in the R channel were 172.67 and 167.68, respectively, and the standard deviations were 28.30 and 46.20, respectively. The average values for the normal and dead cocoons in the G channel were 136.14 and 144.67, respectively, and the standard deviations were 29.25 and 46.70, respectively. In the case of the B channel, the average values were 95.03 and 114.46, respectively, and the standard deviations were 25.64 and 44.65, respectively. Thus, the deviation for the dead cocoon group was greater than that for the normal cocoon group.

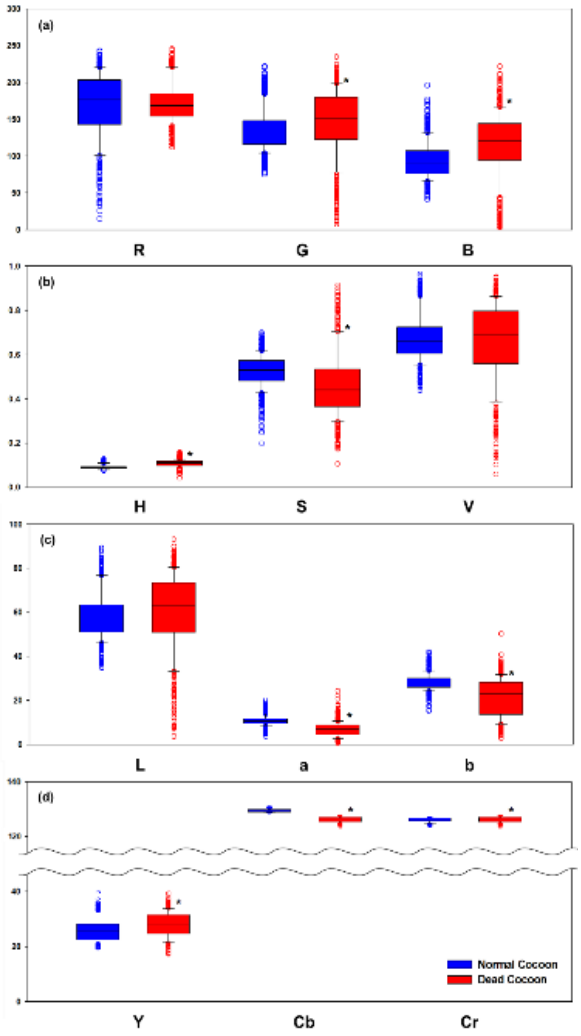

FIGURE 4. Boxplots of mean color values of cocoon groups per color space channel: (a) RGB, (b) HSV, (c) Lab, and (d) YCbCr (p values are significant as per Welch's two sample t-test. *$p < 0.001$.).

The t-test was performed on the normal and dead cocoon groups for each channel. Except for the R channel of the RGB color space, the V channel of the HSV color space, and the L channel of the Lab color space, significant differences were observed, i.e., the p values were 0.001 or lower. Accordingly, it was confirmed that the normal and dead cocoons can be classified based on the color values of the images. However, there was significant overlap between the normal and dead cocoon groups as well as considerable in-group variations. Therefore, it was assumed that the discrimination accuracy based only on the color values of the images would not be high.

B. DISCRIMINATION RESULTS

The k-NN, SVM, LDA, and PLS-DA methods were used on the images composed of the four color spaces, and the results are listed in Table 2. The model was verified by five-fold cross-verification, and the average of five discriminant accuracies was calculated and considered the final discriminant

TABLE 2. Discriminant analyses results for each color space.

		k-NN		SVM		LDA		PLS-DA	
		Cal	Val	Cal	Val	Cal	Val	Cal	Val
RGB	1	95.38	90.09	85.90	87.39	90.76	90.09	77.84	77.93
	2	100	89.76	86.41	89.76	90.01	92.68	76.89	82.44
	3	94.94	81.63	86.90	81.63	91.38	88.27	78.97	73.47
	4	100	86.24	87.03	84.86	90.92	88.99	78.18	77.52
	5	94.17	92.44	85.97	86.67	90.25	91.56	77.65	78.22
	Average	**96.90**	**88.03**	**86.44**	**86.06**	**90.66**	**90.32**	**77.91**	**77.92**
HSV	1	93.60	93.69	93.84	92.79	80.45	84.23	73.22	71.62
	2	94.43	90.73	93.73	91.71	81.07	80.49	72.24	77.07
	3	95.17	89.80	94.02	91.84	81.15	79.08	73.56	71.43
	4	95.99	90.37	93.63	92.66	81.13	80.28	73.00	73.39
	5	93.10	92.89	92.75	95.11	81.33	79.56	73.48	72.44
	Average	**94.46**	**91.50**	**93.59**	**92.82**	**81.03**	**80.73**	**73.10**	**73.19**
Lab	1	91.71	92.79	89.81	90.99	81.52	81.08	77.13	77.93
	2	92.33	91.71	89.66	92.68	80.26	82.44	76.31	82.93
	3	94.14	87.76	91.03	85.71	80.92	79.59	77.70	73.47
	4	94.58	87.61	90.68	88.53	81.72	79.36	80.78	76.61
	5	92.15	90.67	90.01	92.00	80.38	79.56	77.17	79.11
	Average	**92.98**	**90.11**	**90.24**	**89.98**	**80.96**	**80.41**	**77.82**	**78.01**
YCbCr	1	91.11	87.84	88.15	90.09	80.69	82.88	75.71	78.83
	2	92.80	87.80	88.50	87.80	82.46	82.93	75.96	78.05
	3	91.38	88.27	88.62	88.78	83.56	79.08	77.47	72.45
	4	93.63	86.24	89.03	87.16	82.67	81.19	76.30	78.44
	5	90.84	87.11	87.87	87.11	81.93	81.33	77.17	74.22
	Average	**91.95**	**87.45**	**88.43**	**88.19**	**82.26**	**81.48**	**76.52**	**76.40**

performance. All the values were rounded to the third decimal place and the discriminant performance was determined to be the best when the accuracy for the validation group was high.

With respect to the discrimination performances for the different color spaces, the RGB color space showed the highest discrimination accuracy of 90.32% when the LDA method was used. In the case of the HSV and YCbCr color spaces the average accuracies were 92.82% and 88.19%, respectively. For the Lab color space, the k-NN analysis showed a discrimination accuracy of 90.11%. With respect to the discrimination performances for the different types of analysis methods, the k-NN and SVM methods resulted in the highest discrimination accuracies, which were 91.50% and 92.82%, respectively, when the HSV images were used. In the case of the LDA method the discrimination accuracy was 90.32% when the RGB images were used, while in the case of the PLS-DA method, the discrimination accuracy was 78.01% when the Lab images were used. Finally, when the SVM method was used with the HSV color space images, the normal and dead cocoons could be classified with the highest accuracy (92.82%). In the case of PLS-DA, the discrimination accuracy was 80% or less for all the color spaces, in contrast to the other methods. Since PLS-DA is an algorithm suitable for reducing the variable dimension for data such as spectral data, the cocoon classification performance with three input variables was low. For the same reason, since LDA is an algorithm that is used for classification and dimensionality reduction at the same time, LDA showed a lower accuracy than those of k-NN and SVM, which are models that focus on classification.

Before selecting the structure of the lightweight CNN model as shown in Table 1, we conducted an investigation by altering the parameters, as indicated in Table 3. We modified three parameters: the stride size of the convolution layer, pooling type, and the presence of dropout. A total of eight model were compared based on RGB color spaces. Among these, the CNN model, comprising a convolution layer with a stride of 1, max pooling and dropout exhibited the highest performance. Consequently, this model was chosen for the proposed model. It was confirmed that certain parameters did

TABLE 3. Discriminant analyses results of lightweight CNN.

Parameter			Accuracy		
Stride	Pooling	Dropout	Train	Val	Test
1	Max	Y	94.99	95.77	**96.23**
1	Max	N	95.15	96.71	92.52
1	Avg	Y	94.84	94.84	92.52
1	Avg	N	93.11	97.18	94.86
2	Max	Y	87.17	94.37	90.19
2	Max	N	93.74	93.43	92.99
2	Avg	Y	91.86	96.71	92.52
2	Avg	N	96.56	98.12	92.52

not consistently yield better performance, underscoring the importance of finding parameter suitable for the data.

Discrimination models based on deep learning algorithms were then developed to determine whether the performance could be improved compared with that of the existing models. The results are shown in Table 4. The data were randomly divided into training (60%), validation (20%), and test (20%) groups. The training group increased by 16 times using data augmentation. The model training was set to end when the loss of the validation group did not improve for more than 50 consecutive iterations, and the model with the smallest loss in the validation group was considered the final model.

The discrimination accuracy of the proposed lightweight CNN model using the Lab images was 94.21% during training, 96.24% during validation, and 97.66% during the actual test. The discrimination accuracy of the VGG16 model was 97.03% in the case of the training group, 96.71% for the validation group, and 95.79% for the test group, when the Lab images were used. The discrimination accuracy of the ResNet50 model with the Lab images was 97.03% during training, 94.84% during validation, and 96.26% during the actual test. The EfficientNetB0 model yielded a discrimination accuracy of 97.97% in the case of the training group, 97.18% for the validation group, and 97.2% for the test group when the Lab images were used. The discrimination accuracy of the MobileNet model was 96.4% for the training group, 97.65% for the validation group, and 97.2% for the test group when the Lab images were used. The accuracy of the Shuffle Net model was 99.84% for the training group, 89.67% for the validation group and 89.72% for the test group when YCbcr images were used. The GhostNet model yielded a discrimination accuracy of 85.29% in the case of the training group, 84.98% for the validation group, and 94.86% for the test group when the YCbcr images were used. The discrimination accuracy of the ConvNext model using the Lab images was 57.12% during training, 59.15% during validation, and 59.35% during the actual test. Unlike other models, the ConvNext model showed low performances because model learning was not progressed properly. As a result, Lightweight CNN with Lab color spaces demonstrated the highest discrimination accuracy.

SVM exhibited the highest performance when the HSV color space was used, while most CNN models showed high performances in the case of the Lab color space. Particularly, ResNet50 showed little deviation for each color space. It was determined that the ResNet50 model structure included the color space features. Compared to seven transfer learning models, it was confirmed that the proposed model showed high discrimination accuracy in line with previous results.

The lightweight CNN model with the Lab color space was higher than that of the three deep learning models. The lightweight CNN model had a simpler layer structure than other models but yielded the highest performance results. This is because the cocoon image is simple, and it only needs to classify two classes. Hence, a simple structure is sufficient for classification.

The accuracy of the lightweight CNN model was also higher than that of the existing discrimination algorithms (k-NN, SVM, LDA, and PLS-DA). The existing algorithms used three representative values, which were the averages of the color values of all the pixels in a given image, as the variables, whereas the deep learning model used all the pixel values as the variables. It can therefore be concluded that the classification accuracy of the deep learning model was higher because it included the color information based on the positions of the pixels.

Fig. 5 shows the losses for the training and validation groups over epochs for the lightweight CNN model and EfficientNetB0, while Fig. 6 shows the confusion matrix corresponding to these two models. As shown in Fig. 5(a), the lightweight CNN model's epoch was performed 128 times. The loss of the 78-epoch model was 0.1863 during training, 0.1749 during validation, and 0.1348 during the actual test. For the EfficientNetB0 model, the epoch was performed 150 times, and the loss of the 100-epoch model was 0.1319 during training, 0.1368 during validation, and 0.134 during the actual test, as shown in Fig. 5(b). The lightweight CNN model's validation loss steadily decreased, while EfficientNetB0's validation loss varied

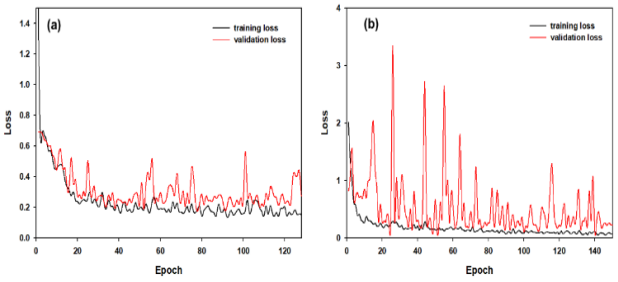

FIGURE 5. Training and validation set losses: (a) Lightweight CNN model with Lab color space images and (b) EfficientNetB0 with Lab color space images.

TABLE 4. Results of discriminant analyses performed using deep learning algorithms based on color spaces.

		RGB	HSV	Lab	YCbCr
Lightweight CNN	Train	94.99	96.56	94.21	59.31
	Validation	95.77	96.71	96.24	59.15
	Test	96.23	95.79	**97.66**	70.09
VGG16	Train	97.65	92.33	97.03	85.29
	Validation	96.24	95.31	96.71	88.73
	Test	94.39	94.86	**95.79**	88.79
ResNet50	Train	93.27	95.31	97.03	94.52
	Validation	92.96	94.37	94.84	92.96
	Test	**96.26**	94.86	**96.26**	**96.26**
EfficientNetB0	Train	95.31	95.31	97.97	97.5
	Validation	94.37	97.18	97.18	96.24
	Test	95.33	95.79	**97.2**	96.73
MobileNet	Train	96.56	94.99	96.4	96.24
	Validation	96.24	97.65	97.65	95.31
	Test	96.73	96.73	**97.2**	92.52
ShuffleNet	Train	97.34	99.53	99.37	99.84
	Validation	91.08	94.37	86.85	89.67
	Test	85.05	88.79	85.05	**89.72**
GhostNet	Train	89.67	94.68	88.58	85.29
	Validation	95.77	96.24	92.49	84.98
	Test	94.39	93.93	93.93	**94.86**
ConvNext	Train	57.59	57.12	57.12	55.71
	Validation	57.28	59.15	59.15	59.15
	Test	54.69	50	**59.35**	50

significantly between epochs. Therefore, we concluded that the lightweight CNN model is more stable than EfficientNetB0.

Table 5 lists the number of parameters and total training time for the deep learning model based on Lab color spaces. Among these, the lightweight CNN model was trained with the fewest parameters, that is, 1,818,498, followed by MobileNet (3,209,026), GhostNet (3,905,856) and ShuffleNet (3,992,670) models. The VGG16 model used approximately 76 times more parameters than the lightweight CNN model. In terms of the total training time, the lightweight CNN model consumed less time at 492 s. MobileNet and GhostNet exhibited a feature of long training time compared with a relatively small number of parameters. ConvNext model consumed the most time, but discriminant accuracy was lowest. Despite the small number of trainable parameters and the short training time, the lightweight CNN model exhibited the highest discrimination accuracy. Therefore, we judged that the proposed Lightweight CNN will be suitable for potential integration into sorting devices.

As shown in the confusion matrix in Fig. 6, both models performed better for classifying the normal cocoons as normal (true positive) than that for classifying the dead cocoons as dead (true negative). The internal shapes of the normal cocoons as observed in the images were usually similar to an oval, whereas the dead cocoons exhibited different shapes. This may be the reason that it was more difficult to classify them compared with the normal cocoons. In the case of the lightweight CNN model, 135 of the 138 normal cocoons and 74 of the 76 dead cocoons were correctly classified in the test dataset, as shown in Fig. 6(a). EfficientNetB0 correctly classified 135 of the 138 normal cocoons and 73 of

TABLE 5. Training time and number of parameters of the models.

Model	Epoch	Trainable Parameter	Total training time (s)
Lightweight CNN	78	1,818,498	492
VGG16	200	138,359,546	1,438
ResNet50	150	23,538,690	1,083
EfficientNetB0	100	4,010,110	727
MobileNet	181	3,209,026	1,280
ShuffleNet	30	3,992,670	366
GhostNet	21	3,905,856	1,413
ConvNext	46	87,568,514	4,820

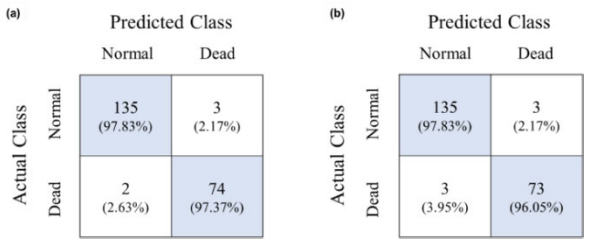

FIGURE 6. Test set confusion matrices: (a) Lightweight CNN model with Lab color space images and (b) EfficientNetB0 with Lab color space images.

the 76 dead cocoons. Hence, the discrimination accuracy between the two models is approximately equal. However, with respect to the number of parameters or model stability, the lightweight CNN is adequate for model training.

To evaluate the robustness of the proposed lightweight CNN model, we conducted 4-fold cross validation. Random partitioning into four groups was performed for all data except the test dataset. Among these groups, three were employed as the training data and one as the validation data, with this process repeated four times by alternating the validation group. The average and standard deviation of accuracy and loss values were computed. The results are presented in Table 6. In the case of accuracy, the standard deviation of 2.51 was observed for the validation dataset, and a small deviation of 0.27 was observed for the test dataset. Similarly, the standard deviation of the loss value was less than 0.06 for all groups. Therefore, we judged that the lightweight CNN model has robustness with respect to data.

Fig. 7 shows the examples of the classification results obtained using CNN models on the test dataset. Fig. 7 (a) depicts the images that were correctly identified as normal cocoons, and Fig. 7 (b) depicts the images of normal cocoons that were erroneously identified as dead cocoons. Fig. 7 (c) comprises the images that were correctly identified as dead cocoons, and Fig. 7 (d) depicts the images of dead cocoons incorrectly identified as normal cocoons. In the case of the cocoons shown in Fig. 7 (b), either their color was not brown, or the cocoons did not maintain their oval shape. The color

TABLE 6. 4-fold cross-validation results of the proposed lightweight CNN.

k	Accuracy			Loss		
	Train	Val	Test	Train	Val	Test
1	95.93	95.77	95.79	0.15	0.15	0.17
2	96.09	96.24	95.79	0.14	0.13	0.15
3	93.74	98.59	96.26	0.18	0.12	0.16
4	95.62	92.49	96.26	0.14	0.26	0.16
average	95.35	95.77	96.03	0.15	0.17	0.16
stdev	1.09	2.51	0.27	0.02	0.06	0.01

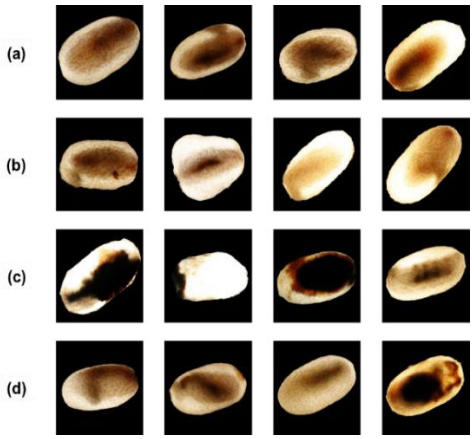

FIGURE 7. Classification results using deep learning algorithms: (a) TP (True Positive), (b) FN (False Negative), (c) TN (True Negative), and (d) FP (False Positive).

of the cocoons shown in Fig. 7(d) was brown and similar to that of normal cocoons. In addition, the pupae within the cocoon maintained an oval shape suggesting that they were mistakenly identified as normal cocoons. In the case of most of the misclassified cases, it was difficult to determine whether the cocoon was normal or dead even with the naked eye. Given this fact, it would be incorrect to ascribe the errors only to the models used. Thus, the deep learning models, particularly the proposed lightweight CNN model, are suitable for discriminating between normal and dead cocoons.

IV. CONCLUSION

In this study, we developed a discrimination model to classify normal and dead cocoons using digital images and various discriminant analysis techniques, including deep learning. A 100 W halogen light was radiated from the above the cocoons in a darkroom and a camera was placed under the cocoons to image them so that the shape of the pupae within the cocoons could be captured. Next, we checked whether the differences between the normal and dead cocoons appeared for each color channel in the RGB, HSV, Lab, and YCbCr color spaces. All the color channel showed significant differences except for the R channel of the RGB space, V channel of the HSV space, and L channel of the Lab space.

Various discriminant algorithms (k-NN, SVM, LDA, and PLS-DA) commonly used for classification were employed to perform discriminant analyses on the normal and dead cocoons based on the color space. When used with the HSV color space images, SVM showed the highest discrimination accuracy of 92.82%. A discrimination model was selected after comparing among the proposed lightweight CNN model and seven state-of-the-art deep learning models. The selected model was the lightweight CNN model, which consisted of six convolutional layers and two fully connected layers. It showed excellent discriminant accuracy, i.e., 94.21% for the training group, 96.24% for the validation group, and 97.66% for the test group.

With respect to the misclassified images most of these images were not easy to discriminate even with the naked eye. Thus, the accuracy of the model in this case was similar to that from manual discrimination. It can be concluded that it is possible to nondestructively classify dead cocoons using images and deep learning techniques.

Our model for classifying dead cocoons showed similar high-discrimination performance to that of several previous state-of-the-art studies However, previous studies were limited to the evaluation of dead cocoons with external defects, whereas our model can identify dead cocoons without external defects. Therefore, the results of our study have superior discrimination performance.

A limitation of this study is that the cocoon images were acquired after removing all the thin threads outside the cocoon. If the model is trained with the cocoon images where these threads are not removed, the discrimination accuracy may decrease. Additionally, the classification model was developed using images of single cocoons. For cocoons produced in a rotating shaft, it would be more effective to develop a model that can detect multiple dead cocoons from a single image. For future work, we plan to develop a model that can detect and discriminate multiple cocoons using a single image. The results of this study provide a foundation for the development of automation technology in the sericulture industry.

REFERENCES

[1] J. C. Russ, *The Image Processing Handbook*, 5th ed. Boca Raton, FL, USA: CRC Press, 2006.

[2] S. R. Dubey and A. S. Jalal, "Apple disease classification using color, texture and shape features from images," *Signal, Image Video Process.*, vol. 10, no. 5, pp. 819–826, Jul. 2016, doi: 10.1007/s11760-015-0821-1.

[3] B. Zhang, W. Huang, L. Gong, J. Li, C. Zhao, C. Liu, and D. Huang, "Computer vision detection of defective apples using automatic lightness correction and weighted RVM classifier," *J. Food Eng.*, vol. 146, pp. 143–151, Feb. 2015, doi: 10.1016/j.jfoodeng.2014.08.024.

[4] J.-G. Park et al., "Techniques for object recognition of image using deep learning," *J. Inst. Control Robot. Syst.*, vol. 21, no. 4, pp. 21–27, 2015.

[5] Y. LeCun, Y. Bengio, and G. Hinton, "Deep learning," *Nature*, vol. 521, no. 7553, pp. 436–444, 2015, doi: 10.1038/nature14539.

[6] L. Alzubaidi, J. Zhang, A. J. Humaidi, A. Al-Dujaili, Y. Duan, O. Al-Shamma, J. Santamaría, M. A. Fadhel, M. Al-Amidie, and L. Farhan, "Review of deep learning: Concepts, CNN architectures, challenges, applications, future directions," *J. Big Data*, vol. 8, no. 1, p. 53, Mar. 2021, doi: 10.1186/s40537-021-00444-8.

[7] V. Tiwari, C. Pandey, A. Dwivedi, and V. Yadav, "Image classification using deep neural network," in *Proc. 2nd Int. Conf. Adv. Comput., Commun. Control Netw. (ICACCCN)*, Dec. 2020, pp. 730–733, doi: 10.1109/ICACCCN51052.2020.9362804.

[8] S. Kuutti, R. Bowden, Y. Jin, P. Barber, and S. Fallah, "A survey of deep learning applications to autonomous vehicle control," *IEEE Trans. Intell. Transp. Syst.*, vol. 22, no. 2, pp. 712–733, Feb. 2021, doi: 10.1109/TITS.2019.2962338.

[9] G. L. Oliveira, A. Valada, C. Bollen, W. Burgard, and T. Brox, "Deep learning for human part discovery in images," in *Proc. IEEE Int. Conf. Robot. Autom. (ICRA)*, May 2016, pp. 1634–1641, doi: 10.1109/ICRA.2016.7487304.

[10] T. E. Potok, C. Schuman, S. Young, R. Patton, F. Spedalieri, J. Liu, K.-T. Yao, G. Rose, and G. Chakma, "A study of complex deep learning networks on high-performance, neuromorphic, and quantum computers," *ACM J. Emerg. Technol. Comput. Syst.*, vol. 14, no. 2, pp. 1–21, Apr. 2018, doi: 10.1145/3178454.

[11] K. Ko, S.-H. Yang, and I. Jang, "Real-time tomato ripeness classification system based on deep learning model for object detection," *J. Inst. Control, Robot. Syst.*, vol. 24, no. 11, pp. 999–1004, Nov. 2018, doi: 10.5302/j.icros.2018.18.0166.

[12] S. Fan, J. Li, Y. Zhang, X. Tian, Q. Wang, X. He, C. Zhang, and W. Huang, "On line detection of defective apples using computer vision system combined with deep learning methods," *J. Food Eng.*, vol. 286, Dec. 2020, Art. no. 110102, doi: 10.1016/j.jfoodeng.2020.110102.

[13] G. L. Grinblat, L. C. Uzal, M. G. Larese, and P. M. Granitto, "Deep learning for plant identification using vein morphological patterns," *Comput. Electron. Agricult.*, vol. 127, pp. 418–424, Sep. 2016, doi: 10.1016/j.compag.2016.07.003.

[14] A. Kaya, A. S. Keceli, C. Catal, H. Y. Yalic, H. Temucin, and B. Tekinerdogan, "Analysis of transfer learning for deep neural network based plant classification models," *Comput. Electron. Agricult.*, vol. 158, pp. 20–29, Mar. 2019, doi: 10.1016/j.compag.2019.01.041.

[15] F. Kurtulmus, W. S. Lee, and A. Vardar, "Immature peach detection in colour images acquired in natural illumination conditions using statistical classifiers and neural network," *Precis. Agricult.*, vol. 15, no. 1, pp. 57–79, Feb. 2014, doi: 10.1007/s11119-013-9323-8.

[16] S. Taghavi Namin, M. Esmaeilzadeh, M. Najafi, T. B. Brown, and J. O. Borevitz, "Deep phenotyping: Deep learning for temporal phenotype/genotype classification," *Plant Methods*, vol. 14, no. 1, p. 66, Dec. 2018, doi: 10.1186/s13007-018-0333-4.

[17] S.-J. Hong, S.-Y. Kim, E. Kim, C.-H. Lee, J.-S. Lee, D.-S. Lee, J. Bang, and G. Kim, "Moth detection from pheromone trap images using deep learning object detectors," *Agriculture*, vol. 10, no. 5, p. 170, May 2020, doi: 10.3390/agriculture10050170.

[18] T. Kasinathan, D. Singaraju, and S. R. Uyyala, "Insect classification and detection in field crops using modern machine learning techniques," *Inf. Process. Agricult.*, vol. 8, no. 3, pp. 446–457, Sep. 2021, doi: 10.1016/j.inpa.2020.09.006.

[19] D. A. B. Oliveira, L. G. R. Pereira, T. Bresolin, R. E. P. Ferreira, and J. R. R. Dorea, "A review of deep learning algorithms for computer vision systems in livestock," *Livestock Sci.*, vol. 253, Nov. 2021, Art. no. 104700, doi: 10.1016/j.livsci.2021.104700.

[20] K.-D. Kwon, A. Lee, J. Lim, S. Cho, W. Lee, B.-K. Cho, and Y. Seo, "Quality grading of Hanwoo (Korean native cattle breed) sub-images using convolutional neural network. Korean," *J. Agric. Sci.*, vol. 47, pp. 1109–1122, 2020, doi: 10.7744/kjoas.20200093.

[21] Z. I. Buhroo, M. A. Bhat, M. A. Malik, A. S. Kamili, N. A. Ganai, and I. L. Khan, "Trends in development and utilization of sericulture resources for diversification and value addition," *Int. J. Entomol. Res.*, vol. 6, no. 1, pp. 27–47, Jun. 2018, doi: 10.33687/entomol.006.01.2069.

[22] K. K. Jaiswal, I. Banerjee, and V. P. Mayookha, "Recent trends in the development and diversification of sericulture natural products for innovative and sustainable applications," *Bioresource Technol. Rep.*, vol. 13, Feb. 2021, Art. no. 100614, doi: 10.1016/j.biteb.2020.100614.

[23] A.-J. Kim et al., "Effect of mulberry fruit tea on the serum lipid profiles and cardiovascular disease markers of middle-aged people living in Choongnam," *J. East Asian Soc. Diet. Life*, vol. 16, no. 4, pp. 408–413, 2006.

[24] H. Kweon et al., "Proximate and nutritional compositions of freeze-dried silkworm powder as edible insect resources," *J. Seric. Entomol. Sci.*, vol. 55, no. 2, pp. 33–39, 2019. [Online]. Available: https://doi.org/10.7852/jses.2019.55.2.33

[25] S. J. Eom, N. H. Lee, M.-C. Kang, Y. H. Kim, T.-G. Lim, and K.-M. Song, "Silk peptide production from whole silkworm cocoon using ultrasound and enzymatic treatment and its suppression of solar ultraviolet-induced skin inflammation," *Ultrason. Sonochemistry*, vol. 61, Mar. 2020, Art. no. 104803, doi: 10.1016/j.ultsonch.2019.104803.
[26] N. Nazim, Z. I. Buhroo, N. Mushtaq, K. Javid, S. Rasool, and G. M. Mir, "Medicinal values of products and by products of sericulture," *J. Pharmacogn. Phytochem.*, vol. 6, pp. 1388–1392, 2017.
[27] Y. Hatano, P. M. Elias, D. Crumrine, K. R. Feingold, K. Katagiri, and S. Fujiwara, "Efficacy of combined peroxisome proliferator-activated receptor-α ligand and glucocorticoid therapy in a murine model of atopic dermatitis," *J. Investigative Dermatology*, vol. 131, no. 9, pp. 1845–1852, Sep. 2011, doi: 10.1038/jid.2011.144.
[28] J.-G. Hwang, J.-K. Yun, K.-H. Han, E.-J. Do, J.-S. Lee, E.-J. Lee, J.-B. Kim, and M.-R. Kim, "Anti-oxidation and antiaging effect of mixed extract from Korean medicinal herbs," *Kor J. Herbol.*, vol. 26, no. 1, pp. 111–117, 2011, doi: 10.6116/kjh.2011.26.1.111.
[29] S.-K. Kim, Y.-Y. Jo, K.-G. Lee, K.-Y. Kim, H.-B. Kim, and H. Kweon, "Effect of ethanol concentration on the infrared spectroscopic characteristics of silk beads," *J. Sericultural Entomol. Sci.*, vol. 53, no. 2, pp. 118–123, Oct. 2015, doi: 10.7852/jses.2015.53.2.118.
[30] S.-H. Lim et al., *Sericulture Training Manual*. FAO, Agricult. Services, Rome, Italy, 1990.
[31] T. N. Sonwalkar, *Hand Book of Silk Technology*. New York, NY, USA: Taylor & Francis, 1993.
[32] P. P. Prasobhkumar, C. R. Francis, and S. S. Gorthi, "Cocoon quality assessment system using vibration impact acoustic emission processing," *Eng. Agricult., Environ. Food*, vol. 12, no. 4, pp. 556–563, Oct. 2019, doi: 10.1016/j.eaef.2019.11.008.
[33] J.-R. Cai, L.-M. Yuan, B. Liu, and L. Sun, "Nondestructive gender identification of silkworm cocoons using X-ray imaging with multivariate data analysis," *Anal. Methods*, vol. 6, no. 18, pp. 7224–7233, 2014, doi: 10.1039/c4ay00940a.
[34] F. Dai, X. Wang, Y. Zhong, S. Zhong, and C. Chen, "Convolution neural network application in the simultaneous detection of gender and variety of silkworm (Bombyx mori) cocoons," *J. Phys., Conf. Ser.*, vol. 1769, no. 1, Jan. 2021, Art. no. 012017, doi: 10.1088/1742-6596/1769/1/012017.
[35] S. Thomas and J. Thomas, "A review on existing methods and classification algorithms used for sex determination of silkworm in sericulture," in *Intelligent Systems Design and Applications*, A. Abraham, V. Piuri, N. Gandhi, P. Siarry, A. Kaklauskas and A. Madureira, Eds. Cham, Switzerland: Springer, 2021, pp. 567–579, doi: 10.1007/978-3-030-71187-0_52.
[36] D. Tao, Z. Wang, G. Li, and G. Qiu, "Accurate identification of the sex and species of silkworm pupae using near infrared spectroscopy," *J. Appl. Spectrosc.*, vol. 85, no. 5, pp. 949–952, Nov. 2018, doi: 10.1007/s10812-018-0744-z.
[37] Z. Zhu, H. Yuan, C. Song, X. Li, D. Fang, Z. Guo, X. Zhu, W. Liu, and G. Yan, "High-speed sex identification and sorting of living silkworm pupae using near-infrared spectroscopy combined with chemometrics," *Sens. Actuators B, Chem.*, vol. 268, pp. 299–309, Sep. 2018, doi: 10.1016/j.snb.2018.04.093.
[38] H. Zheng, "Research on image preprocessing of silkworm cocoon based on machine vision," in *Proc. 3rd Int. Conf. Mech., Control Comput. Eng. (ICMCCE)*, Sep. 2018, pp. 640–642, doi: 10.1109/ICMCCE.2018.00141.
[39] P. P. Prasobhkumar, C. R. Francis, and S. S. Gorthi, "Automated quality assessment of cocoons using a smart camera based system," *Eng. Agricult., Environ. Food*, vol. 11, no. 4, pp. 202–210, Oct. 2018, doi: 10.1016/j.eaef.2018.05.002.
[40] W. Feng, G. Jia, W. Wang, Z. Zhang, J. Cui, Z. Chu, and B. Xu, "A lightweight convolutional neural network for silkworm cocoons fast classification," in *Cognitive Systems and Signal Processing*, F. Sun, H. Liu, and D. Hu, Eds. Singapore: Springer, 2019, pp. 301–309, doi: 10.1007/978-981-13-7986-4_27.
[41] W. Sun, Z. Huang, M. Liang, T. Shao, and H. Bi, "Cocoon image segmentation method based on fully convolutional networks," in *Proc. 7th Asia Int. Symp. Mechatronics*, B. Duan, K. Umeda, and W. Hwang, Eds. Singapore: Springer, 2020, pp. 832–843, doi: 10.1007/978-981-32-9441-7_85.
[42] N. Otsu, "A threshold selection method from gray-level histograms," *IEEE Trans. Syst., Man, Cybern.*, vol. 9, no. 1, pp. 62–66, 1979.

AHYEONG LEE received the Ph.D. degree in biosystems engineering from Seoul National University, Seoul, Republic of Korea, in 2023. She is a Researcher with the Department of Agricultural Engineering, National Institute of Agricultural Sciences, Rural Development Administration, Republic of Korea. Her research interests include non-destructive analyses, image processing, and spectral analyses.

GIYOUNG KIM received the Ph.D. degree in biosystems engineering from Virginia Polytechnic Institute and State University, Blacksburg, VA, USA, in 1995. He is currently a Senior Researcher with the Department of Agricultural Engineering, National Institute of Agricultural Sciences, Rural Development Administration, Republic of Korea. His research interests include rapid detection methods, biosensors, machine vision, and digital HACCP management systems for food safety.

SUK-JU HONG received the Ph.D. degree in biosystems engineering from Seoul National University, Seoul, Republic of Korea, in 2022. He is a Postdoctoral Researcher with the Department of Agricultural Engineering, National Institute of Agricultural Sciences, Rural Development Administration, Republic of Korea. His research interests include non-destructive testing, image processing, and deep learning applications in agriculture.

SEONG-WAN KIM received the Ph.D. degree in medicine from Chungnam National University, Daejeon, Republic of Korea, in 2009. He is currently a Researcher with the Department of Agricultural Biology, National Institute of Agricultural Sciences, Rural Development Administration, Republic of Korea. His research interests include silkworm breeding study, insect molecular biology, and silkworm transformation.

GHISEOK KIM received the Ph.D. degree in agricultural machinery engineering from Chungnam National University, South Korea, in 2007. From 2009 to 2011, he was a Research Scientist with the Composite Vehicle Research Center, Michigan State University, USA. From 2011 to 2015, he was a Research Scientist with the Optical Analysis Equipment Development Team, Korea Basic Science Institute. He is currently an Associate Professor with the Department of Biosystems Engineering, Seoul National University, Seoul, Republic of Korea. His research interests include analysis of physical and engineering properties of agricultural products, development of postharvest process engineering techniques, and research on nondestructive evaluation of agricultural products including meat and fishery.